Supplementary Information

Tetranuclear-cluster-based MOF with low-polar pore environment for efficient C_2H_6/C_2H_4 separation

Meng Feng[a], Jiantang Li[a], Xirong Wang[a], Jingyu Wang[a], Dongmei Wang*[a] and Banglin Chen*[ab]

[a] Key Laboratory of the Ministry of Education for Advanced Catalysis Materials, College of Chemistry and Materials Sciences, Zhejiang Normal University, Jinhua 321004 (P. R. China). E-mail: dmwang@zjnu.edu.cn

[b] Fujian Key Laboratory of Polymer Materials, College of Chemistry and Materials Sciences, Fujian Normal University, Fujian, 350007, P. R. China. E-mail: banglin.chen@fjnu.edu.cn

Calculation procedures of selectivity from IAST

The measured experimental data is excess loadings (q^{ex}) of the pure components C_2H_2, C_2H_6 and C_2H_4 for ZJNU-400, which should be converted to absolute loadings (q) firstly.

$$q = q^{ex} + \frac{pV_{pore}}{ZRT} \quad \text{(S1)}$$

Here Z is the compressibility factor. The Peng-Robinson equation was used to estimate the value of compressibility factor to obtain the absolute loading, while the measure pore volume is also necessary.

In order to perform the IAST calculations, the single-component isotherm was fitted by the dual-site Langmuir-Freundlich (DSLF) adsorption model to correlate the pure-component equilibrium data and further predict the adsorption of mixtures. The DSLF model is described as:

$$q = q_{m_1} \times \frac{b_1 \times p^{1/n_1}}{1+b_1 \times p^{1/n_1}} + q_{m_2} \times \frac{b_2 \times p^{1/n_2}}{1+b_2 \times p^{1/n_2}} \quad \text{(S2)}$$

Here p is the pressure of the bulk gas at equilibrium with the adsorbed phase (kPa), q is the adsorbed amount per mass of adsorbent (mol kg^{-1}), q_{m1} and q_{m2} are the saturation capacities of sites 1 and 2 (mol kg^{-1}), b_1 and b_2 are the affinity coefficients of sites 1 and 2 (1/kPa), n_1 and n_2 are the deviations from an ideal homogeneous surface. To investigate the separation of binary mixtures, the adsorption selectivity is defined by

$$S_{ij} = \frac{x_1 / x_2}{y_1 / y_2} \quad \text{(S3)}$$

x_1 and x_2 are the absolute component loadings of the adsorbed phase in the mixture. These component loadings are also termed the uptake capacities. We calculate the values of x_1 and x_2 using the Ideal Adsorbed Solution Theory (IAST) of Myers and Prausnitz.

S1. Supporting Figures

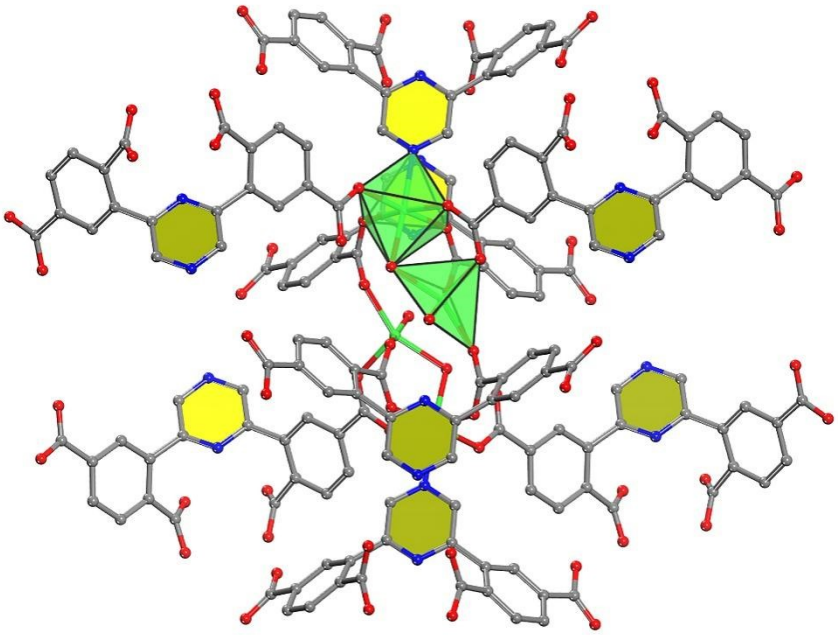

Fig S1. Coordinated environment of tetranuclear manganese cluster.

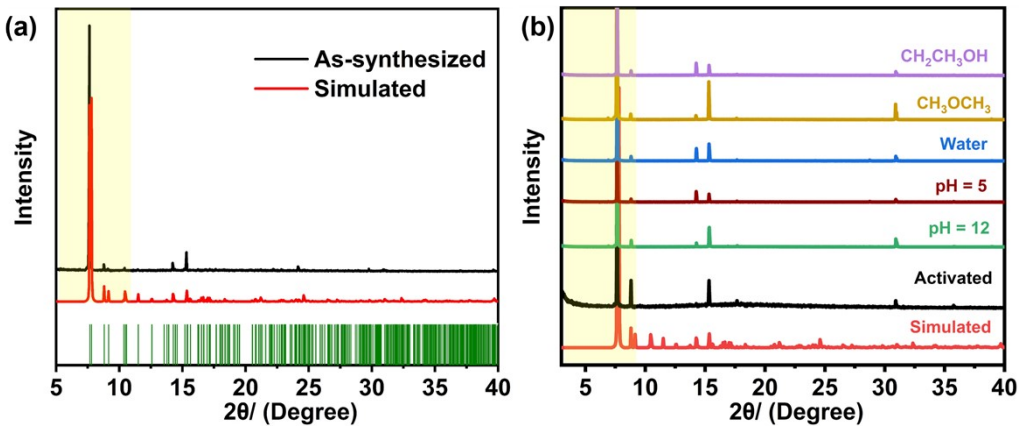

Fig S2. PXRD patterns of ZJNU-400 for simulated, as-synthesized and PXRD of in water and some organic solvent for three days.

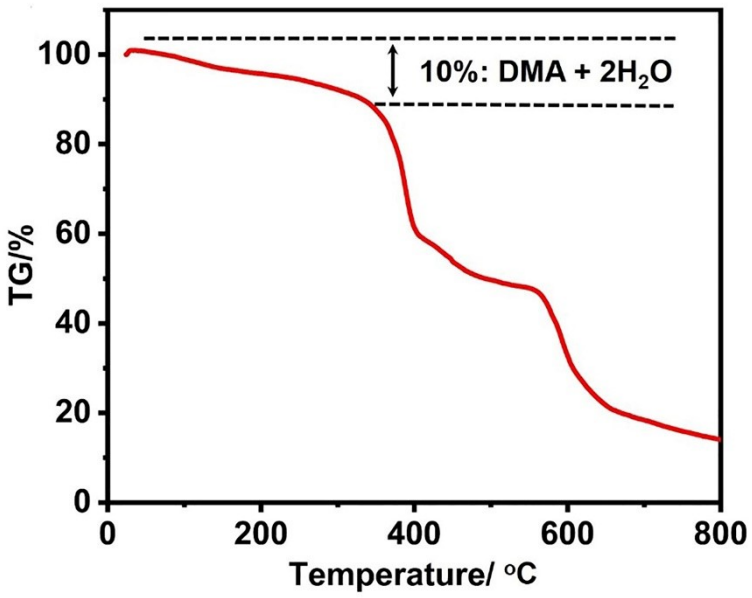

Fig S3. Thermogravimetric analysis curve of ZJNU-400 for the as-synthesized sample.

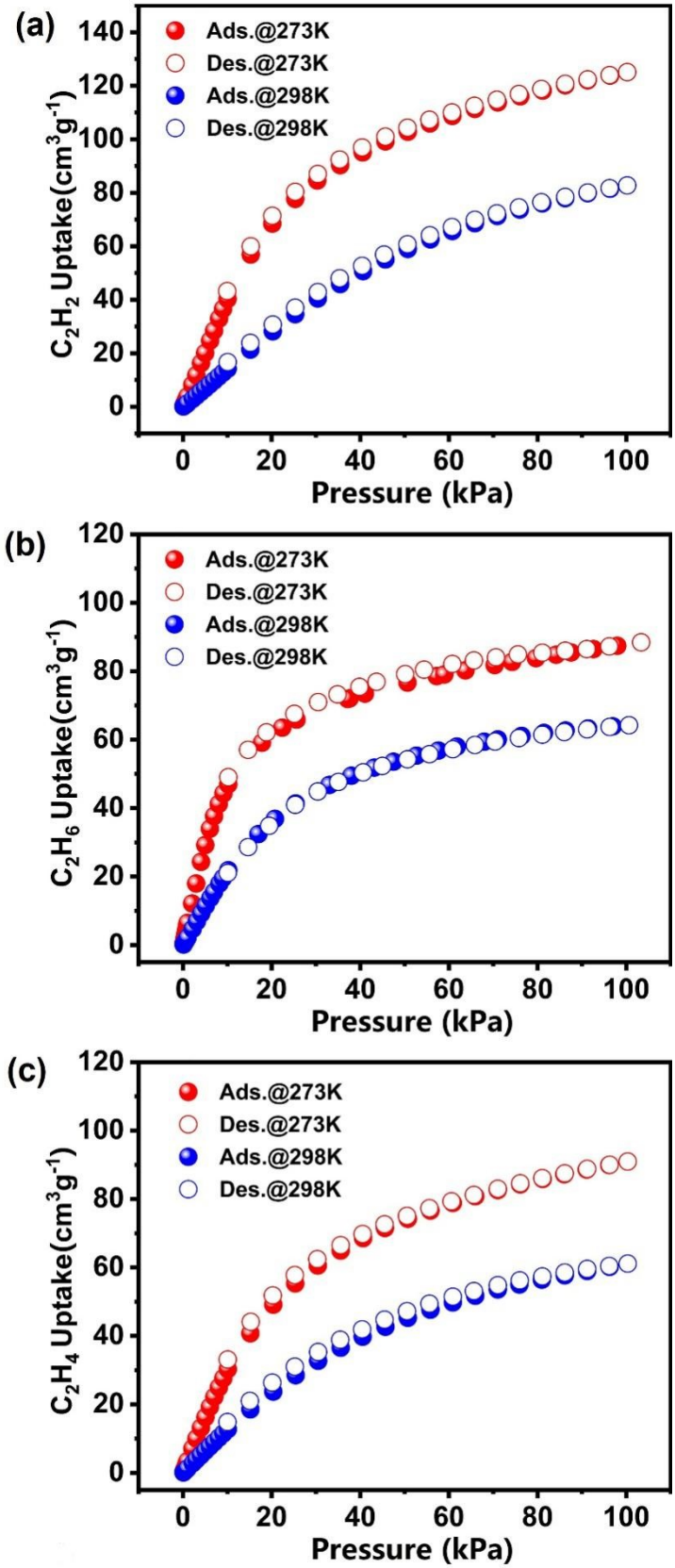

Fig S4. (a) C_2H_2, (b) C_2H_6, and (c) C_2H_4 adsorption and desorption isotherms of ZJNU-400.

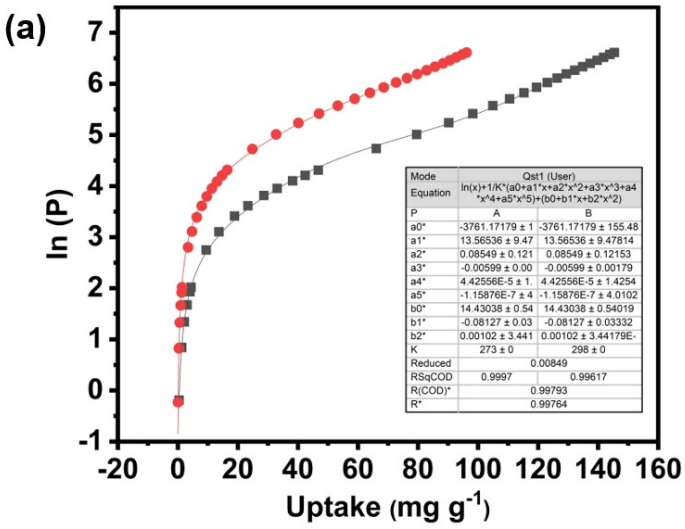

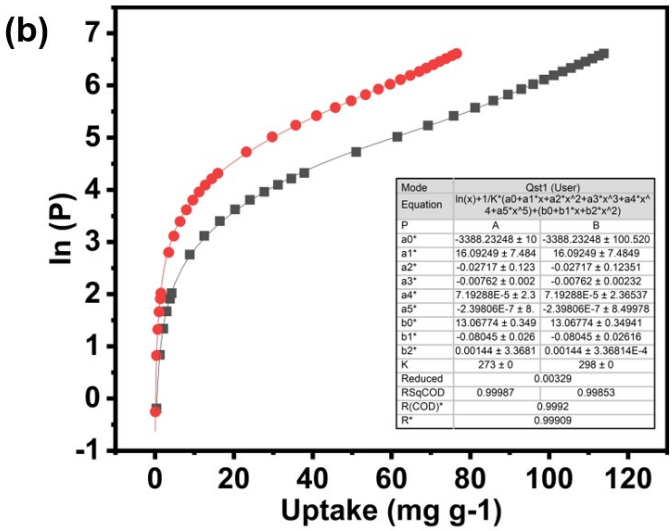

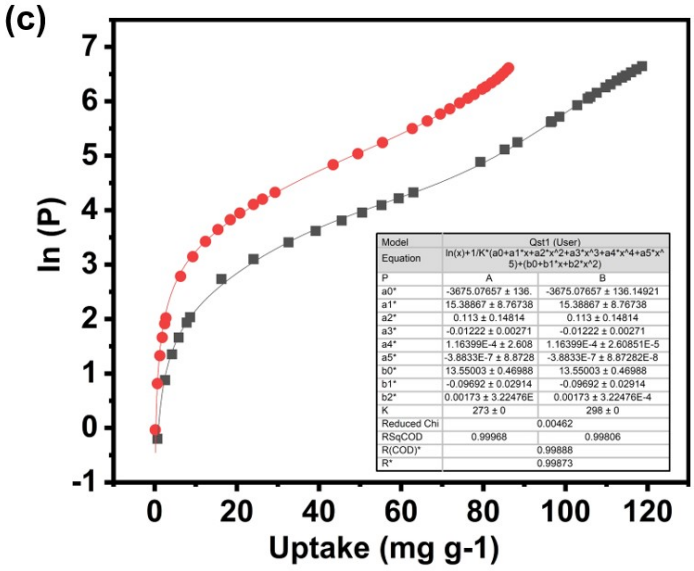

Fig S5. The fitting results of Q_{st} for (a) C_2H_2, (b) C_2H_4, (c) C_2H_6 on ZJNU-400 by using adsorption isotherms at 273 K and 298 K**.**

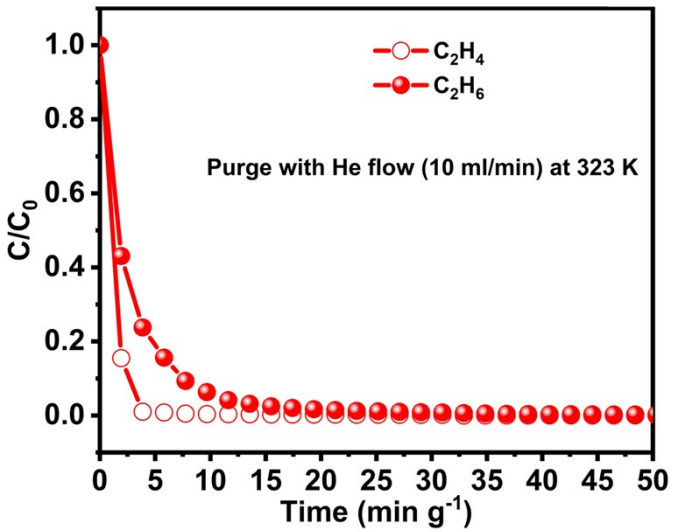

Fig S6. The desorption curves were recorded on the column at 50 °C under He flow of 10 mL min^{-1}.

S2. Supporting Tables

Table S1. Crystal data and structure refinement for ZJNU-400.

MOF	ZJNU-400
Empirical formula	$C_{20}H_{12}Mn_2N_2O_{10}$
Formula weight	550.20
Wavelength (Å)	0.71073
Crystal system	Monoclinic
Space group	$P2_1/n$
a (Å)	15.3929(5)
b (Å)	12.4098(5)
c (Å)	17.0932(7)
α (º)	90
β (º)	90.9600(10)
γ (º)	90
Volume (Å^3)	3264.7(2)
Z	4
Dc (g/cm^3)	1.119
μ (mm^{-1})	0.814
F (000)	1104.0
Reflections collected	32743
Unique (R_{int})	7465(0.0289)
Goodness-of-fit on F^2	1.045
R_1, wR_2 [I>2σ(I)]	0.0238, 0.0650
R_1, wR_2 (all data)	0.0284, 0.0672
Largest diff. peak and hole (e/Å^3)	0.34/-0.22

The guest molecules were highly disordered and could not be modeled properly, thus the SQUEEZE routine of PLATON was applied to remove the contributions to the scattering from the solvent molecules. The reported refinements are of the guest-free structures using the *.hkp files produced using the SQUEEZE routine.

Table S2. The refined parameters for the Dual-site Langmuir-Freundlich equations fit for the pure isotherms of small gas molecule for ZJNU-400 at 298 K.

Adsorbate	q_{m1} [mmol g^{-1}]	b_1 [kPa^{-1}]	n_1	q_{m2} [mmol g^{-1}]	b_2 [kPa^{-1}]	n_2	R^2
C_2H_2	4.50407	0.0037	1.4211	0.50000	0.0834	1.0000	1.0000
C_2H_4	0.08199	0.3274	1.0986	3.65780	0.0094	1.2203	1.0000
C_2H_6	1.14899	0.0137	1.5495	2.31735	0.0336	1.0000	1.0000

Table S3. C_2H_6/C_2H_4 (298K, 50:50) selectivity performance comparison of some previous reported MOFs.

Compound	C_2H_6 uptake ($cm^3\ g^{-1}$)	Sel. C_2H_6/C_2H_4 (v:v 50:50)	Reference
ZJNU-400	**64**	**2.8**	**This work**
STU-1	74.1	1.5	1
ZUL-C4	65.6	2.2	2
UiO-66-2Me	48.16	2.9	3
MOF-808-Bzz	49.28	1.9	4
NKU-200-Tb	60.25	2.1	5
Co-9-ina	84	2.7	6
BUT-150	96.3	1.15	7
Y-TATB	97.0	1.8	8
JNU-6-CH3	103.7	2.2	9
JNU-6	113.6	1.9	9
UIO-67-(NH2)2[a]	119.2	1.7	10
MAF-49	38.5	2.7	11
Ni-MOF 2	133	1.9	12
Co-TATB[a]	72.35	1.4	13
Ni(bdc)(ted)0.5	112	2.0	14
UTSA-30	47	3.8	15
$Fe_2(O_2)$(dobdc)	73.7	4.4	16
$Cu(Qc)_2$	41.4	3.4	17
$Co(AIN_{)2}$	70.9	2.9	18
UiO-66-2CF_3	19.2	2.5	19
ZIF-4	51.5	2.1	20
MUF-15	105.0	1.9	21
IRMOF-8	112.4	1.8	22
ZJU-121a	69.4	1.5	23
Azole-Th-1	100.2	1.4	24
UTSA-35	54.4	1.4	25
MIL-53(Al)	45.9	1.3	26
TJT-100	79	1.2	27
LIFM-28	22.4	1.1	28

[a]C_2H_6, C_2H_4 uptake, uptake ratio and IAST selectivity were all measured at 296 K.

References

1. D. Luo, Y.-L. Peng, M. Xie, M. Li, A. A. Bezrukov, T. Zuo, X.-Z. Wang, Y. Wu, Y. Y. Li, A. R. Lowe, M. a. Chorążewski, Y. Grosu, Z. Zhang, M. J. Zaworotko, X.-P. Zhou and D. Li, Improving ethane/ethylene separation performance under humid conditions by spatially modified zeolitic imidazolate frameworks, ACS Appl. Mater. Interfaces, 2022, 14, 11547-11558.
2. J. Zhou, T. Ke, X. Zhu, B. Jin, Z. Bao, Z. Zhang, Y. Yang, Q. Ren and Q. Yang, Combination of low-polar and polar binding sites in aliphatic mofs for the efficient c2h6/c2h4 separation, ACS Appl. Mater. Interfaces, 2023, 15, 3387-3394.
3. W. Park, T.-H. Kim, K. Hyun Oh, H. Hee Han, Y. Choi, K. Kim and Y.-S. Bae, High C_2H_4/ C_2H_6 selectivity via incorporation of dense methyl groups into a stable zr-based mof with cavity-like pores, Chem. Eng. J., 2024, 481, 148707.
4. C. Song, F. Zheng, Y. Liu, Q. Yang, Z. Zhang, Q. Ren and Z. Bao, Spatial distribution of nitrogen binding sites in metal-organic frameworks for selective ethane adsorption and one-step ethylene purification, Angew. Chem. Int. Ed., 2023, 62, e202313855.
5. J.-J. Pang, Z.-H. Ma, Q.-Q. Yang, K. Zhang, X. Lian, H. Huang, Z.-Q. Yao, B. Li, J. Xu and X.-H. Bu, A highly connected metal–organic framework with a specific nonpolar nanotrap for inverse ethane/ethylene separation, Inorg. Chem. Front., 2023, 10, 6407-6413.
6. S.-M. Wang, H.-R. Liu, S.-T. Zheng, H.-L. Lan, Q.-Y. Yang and Y.-Z. Zheng, Control of pore structure by the solvent effect for efficient ethane/ethylene separation, Sep. Purif. Technol., 2023, 304, 122378.
7. H.-T. Wang, Q. Chen, X. Zhang, Y.-L. Zhao, M.-M. Xu, R.-B. Lin, H. Huang, L.-H. Xie and J.-R. Li, Two isostructural metal–organic frameworks with unique nickel clusters for c2h2/c2h6/c2h4 mixture separation, J. Mater. Chem. A, 2022, 10, 12497-12502.
8. S. Zhao, J. Yao, Q. Fan, Y. Yuan, S. Tu, Y. Wu and Q. Xia, A highly stable yttrium-based metal-organic framework with two-fold interpenetrated and cage-like pore structure for one-step purification of ethylene from ethylene/ethane mixture, Sep. Purif. Technol., 2024, 330, 125256.
9. X.-J. Xie, Y. Wang, Q.-Y. Cao, R. Krishna, H. Zeng, W. Lu and D. Li, Surface engineering on a microporous metal–organic framework to boost ethane/ethylene separation under humid conditions, Chem. Sci., 2023, 14, 11890-11895.
10. X.-W. Gu, J.-X. Wang, E. Wu, H. Wu, W. Zhou, G. Qian, B. Chen and B. Li, Immobilization of lewis basic sites into a stable ethane-selective mof enabling one-step separation of ethylene from a ternary mixture, J. Am. Chem. Soc., 2022, 144, 2614-2623.
11. P.-Q. Liao, W.-X. Zhang, J.-P. Zhang and X.-M. Chen, Efficient purification of ethene by an ethane-trapping metal-organic framework, Nat. Commun., 2015, 6, 8697.
12. Y. Ye, Y. Xie, Y. Shi, L. Gong, J. Phipps, A. M. Al-Enizi, A. Nafady, B. Chen and S. Ma, A microporous metal-organic framework with unique aromatic pore surfaces for high performance c2h6/c2h4 separation, Angew. Chem. Int. Ed., 2023, 62, e202302564.
13. L. Liu, Y. Bo, W. Zhuang, Z. Xie, Y. Yang, Q. Lin, D. Chen, Z. Yao and S. Xiang, A microporous metal-organic framework with channels constructed from nonpolar aromatic rings for the selective separation of ethane/ethylene mixtures, ChemPlusChem, 2022, 87, e202100482.
14. W. Liang, F. Xu, X. Zhou, J. Xiao, Q. Xia, Y. Li and Z. Li, Ethane selective adsorbent ni(bdc)(ted)0.5 with high uptake and its significance in adsorption separation of ethane and ethylene, Chem. Eng. Sci., 2016, 148, 275-281.
15. Y. He, S. Xiang, Z. Zhang, S. Xiong, F. R. Fronczek, R. Krishna, M. O'Keeffe and B. Chen,

A microporous lanthanide-tricarboxylate framework with the potential for purification of natural gas, Chem. Commun., 2012, 48, 10856-10858.
16. L. Li, R.-B. Lin, R. Krishna, H. Li, S. Xiang, H. Wu, J. Li, W. Zhou and B. Chen, Ethane/ethylene separation in a metal-organic framework with iron-peroxo sites, Science, 2018, 362, 443-446.
17. R.-B. Lin, H. Wu, L. Li, X.-L. Tang, Z. Li, J. Gao, H. Cui, W. Zhou and B. Chen, Boosting Ethane/Ethylene Separation within Isoreticular Ultramicroporous Metal–Organic Frameworks, J. Am. Chem. Soc., 2018, 140, 12940-12946.
18. M. Kang, D. W. Kang, J. H. Choe, H. Kim, D. W. Kim, H. Park and C. S. Hong, A Robust Hydrogen-Bonded Metal–Organic Framework with Enhanced Ethane Uptake and Selectivity, Chem. Mater., 2021, 33, 6193-6199.
19. J. Pires, J. Fernandes, K. Dedecker, J. R. B. Gomes, G. Pérez-Sánchez, F. Nouar, C. Serre and M. L. Pinto, Enhancement of Ethane Selectivity in Ethane–Ethylene Mixtures by Perfluoro Groups in Zr-Based Metal-Organic Frameworks, ACS Appl. Mater. Interfaces, 2019, 11, 27410-27421.
20. M. Hartmann, U. Böhme, M. Hovestadt and C. Paula, Adsorptive Separation of Olefin/Paraffin Mixtures with ZIF-4, Langmuir, 2015, 31, 12382-12389.
21. O. T. Qazvini, R. Babarao, Z.-L. Shi, Y.-B. Zhang and S. G. Telfer, A Robust Ethane-Trapping Metal–Organic Framework with a High Capacity for Ethylene Purification, J. Am. Chem. Soc., 2019, 141, 5014-5020.
22. J. Pires, M. L. Pinto and V. K. Saini, Ethane Selective IRMOF-8 and Its Significance in Ethane–Ethylene Separation by Adsorption, ACS Appl. Mater. Interfaces, 2014, 6, 12093-12099.
23. J. Pei, J.-X. Wang, K. Shao, Y. Yang, Y. Cui, H. Wu, W. Zhou, B. Li and G. Qian, Engineering microporous ethane-trapping metal–organic frameworks for boosting ethane/ethylene separation, J. Mater. Chem., 2020, 8, 3613-3620.
24. Z. Xu, X. Xiong, J. Xiong, R. Krishna, L. Li, Y. Fan, F. Luo and B. Chen, A robust Th-azole framework for highly efficient purification of C_2H_4 from a $C_2H_4/C_2H_2/C_2H_6$ mixture, Nat. Commun., 2020, 11, 3163.
25. Y. He, Z. Zhang, S. Xiang, F. R. Fronczek, R. Krishna and B. Chen, A robust doubly interpenetrated metal–organic framework constructed from a novel aromatic tricarboxylate for highly selective separation of small hydrocarbons, Chem. Commun., 2012, 48, 6493-6495.
26. R. P. P. L. Ribeiro, B. C. R. Camacho, A. Lyubchyk, I. A. A. C. Esteves, F. J. A. L. Cruz and J. P. B. Mota, Experimental and computational study of ethane and ethylene adsorption in the MIL-53(Al) metal organic framework, Microporous Mesoporous Mater., 2016, 230, 154-165.
27. H.-G. Hao, Y.-F. Zhao, D.-M. Chen, J.-M. Yu, K. Tan, S. Ma, Y. Chabal, Z.-M. Zhang, J.-M. Dou, Z.-H. Xiao, G. Day, H.-C. Zhou and T.-B. Lu, Simultaneous Trapping of C_2H_2 and C_2H_6 from a Ternary Mixture of $C_2H_4/C_2H_2/C_2H_6$ in a Robust Metal–Organic Framework for the Purification of C_2H_4, Angew. Chem. Int. Ed., 2018, 57, 16067-16071.
28. C.-X. Chen, Z.-W. Wei, T. Pham, P. C. Lan, L. Zhang, K. A. Forrest, S. Chen, A. M. Al-Enizi, A. Nafady, C.-Y. Su and S. Ma, Nanospace Engineering of Metal–Organic Frameworks through Dynamic Spacer Installation of Multifunctionalities for Efficient Separation of Ethane from Ethane/Ethylene Mixtures, Angew. Chem. Int. Ed., 2021, 60, 9680-9685.